ELSEVIER

Polymer Degradation and Stability 80 (2003) 127–134

Polymer Degradation and Stability

www.elsevier.com/locate/polydegstab

Physical properties and biodegradability of maleated-polycaprolactone/starch composite

Chin-San Wu*

Department of Chemical Engineering, Kao Yuan Institute of Technology, Kaohsiung County, Taiwan 82101, Republic of China

Received 7 October 2002; accepted 15 November 2002

Abstract

The properties of blends of polycaprolactone and starch (PCL/starch) and maleic anhydride (MAH)-grafted-polycaprolactone and starch (PCL-g-MAH/starch) were examined using Fourier transform infrared (FTIR) spectroscopy, ^{1}H nuclear magnetic resonance (^{1}H NMR), differential scanning calorimetry (DSC), and mechanical testing. Mechanical and thermal properties of PCL became noticeably worse when it was blended with starch, due to the poor compatibility between the two phases. The greater compatibility of PCL-g-MAH with starch, owing to the formation of an ester carbonyl group, led to a much better dispersion and homogeneity of starch in the PCL-g-MAH matrix and consequently to noticeably better properties. Furthermore, with a lower melt temperature, the PCL-g-MAH/starch blend is more easily processed than PCL/starch. Both blends were buried in soil to assess biodegradability. Water resistance of PCL-g-MAH/starch was higher than that of PCL/starch, although weight loss of blends buried in soil indicated that both were biodegradable, even at high levels of starch substitution. In soil, the mechanical properties of both blends, such as tensile strength and elongation at break, also deteriorated.

Keywords: Blends; PCL-g-MAH/starch; Mechanical and thermal properties; Biodegradability

1. Introduction

The non-biodegradability of most plastics has caused many environmental problems associated with their disposal. Recycling is an environmentally attractive solution. However, only a minor portion of plastics is recyclable, and most end up in municipal burial sites. This leads to the increasingly difficult problem of finding available landfill areas. Hence, to reduce the dependence on landfills, there has been an increased interest in the production and use of biodegradable polymers. Among the commercially available biodegradable plastics, polycaprolactone (PCL) has received much attention due to its high flexibility and biodegradability and because of its hydrophobic nature. PCL is, however, too expensive to be used widely.

In the past decades, many attempts have been focused on blending plastic materials with cheap and biodegradable natural biopolymers, such as starch, cellulose, and chitin, to create new materials with desired properties [1–12]. These biopolymers, especially starch, are abundant, inexpensive, renewable, and fully biodegradable. However, in addition to being susceptible to water absorption, blends of biopolymer and polymer exhibit inferior mechanical properties because the hydrophilic character of the biopolymer leads to poor adhesion with the hydrophobic polymer. A feasible solution is to use PCL as the matrix material and biopolymer as a modulus-modifier and extender, and this has been discussed in some detail elsewhere. Nevertheless, physical properties of PCL become significantly worse when blended with starch due to the poor compatibility between the two phases. Such an operation therefore requires a compatibilizer and/or a toughener to enhance the compatibility between the two immiscible phases and to improve the mechanical properties of the composite [13]. Studies by Bikiaris and Panayiotou [14] showed that maleic anhydride-grafted-polyethylene (PE-g-MAH) increased the compatibility between low-density polyethylene (LDPE)

* Corresponding author. Tel.: +886-7-6968121; fax: +886-7-6968128.

E-mail address: cws1222@cc.kyit.edu.tw (C.-San Wu).

0141-3910/03/$ - see front matter © 2003 Elsevier Science Ltd. All rights reserved.
doi:10.1016/S0141-3910(02)00393-2

and plasticized starch. This suggests that the blending of PCL with the cheaper material starch, with a reactive functional group grafted onto PCL to improve adhesion and dispersion of the two immiscible phases, offers the best combination of cheapness and good mechanical properties [15,16].

In this study, we systematically investigated the effect of replacing pure PCL with maleic anhydride-grafted-PCL (PCL-g-MAH), synthesized in our laboratory, on structure and properties of PCL/starch-type composites. The composites were characterized using FTIR spectroscopy, ^{1}H nuclear magnetic resonance (^{1}H NMR), and differential scanning calorimetry (DSC) to identify the structural changes caused by the grafting of maleic anhydride. Scanning electron microscopy (SEM) and mechanical testing were also used to examine morphology and mechanical properties of blends. Additionally, water absorption of synthesized blends and weight loss of buried blends was estimated to assess water resistance and biodegradability.

2. Experimental

2.1. Materials

Polycaprolactone (molar mass 80,000 g/mol) was supplied by Solvay, and starch (27% amylose and 73% amylopectin) by Sigma Chemical Corporation. Maleic anhydride, a commercial product of Aldrich, was purified by re-crystallization with chloroform before use. Benzoyl peroxide (BPO) was used as initiator and was purified by dissolving in chloroform and reprecipitating with methanol. The PCL-g-MAH copolymer was prepared in our laboratory via the procedures described in the following section.

2.2. Sample preparation

2.2.1. Graft reaction and sample preparation

Four equal portions of maleic anhydride and benzoyl peroxide mixture were added into molten PCL stepwise at 2-min intervals. The reactions were carried out under nitrogen at 85±2 °C. In preliminary experiments, it was found that reaction equilibrium could be attained after 5 h. Nevertheless, to be sure that equilibrium was established, all the reactions were run for 6 h, at a rotor speed of 60 rpm. The grafted product (4g) was then dissolved in 200 ml refluxing xylene at 85 °C and the hot solution filtered through several layers of cheesecloth. The cheesecloth was washed with acetone to remove the xylene-insoluble unreacted maleic anhydride and the product remaining over the cheesecloth was dried in a vacuum oven at 80 °C for 24 h. The xylene-soluble product in the filtrate was extracted five times, using 600 ml cold acetone for each extraction. Subsequently, the grafting percentage was determined, using a titration method [17].

2.2.2. Determination of grafting percentage

Maleic anhydride loading of the xylene-soluble polymer (expressed as grafting percentage) was calculated from the acid number and was determined as follows: Firstly, about 2 g of copolymer was heated in 200 ml of refluxing xylene for 2 h. The hot solution was then titrated immediately with a 0.03 N ethanolic KOH solution, which was standardized against a solution of potassium hydrogen phthalate, with phenolphthalein used as an indicator. The acid number was calculated using Eq. (1) below, and the grafting percentage calculated using Eq. (2) [17].

$$\text{Acid number (mgKOH/g)} = \frac{\text{VKOH (ml)} \times C_{KOH}\ \text{(N)} \times 56.1}{\text{polymer (g)}} \quad (1)$$

$$\text{Grafting percentage (\%)} = \frac{\text{Acid number} \times 98.1}{2 \times 561} \times 100\% \quad (2)$$

Grafting percentage was found to be about 0.98 wt.% when BPO loading was maintained at 0.3 wt.% and MAH loading was maintained at 10 wt.%.

2.2.3. Blend preparation

All the blends were prepared using a Brabender "Plastograph" W50EHT 200Nm mixer with a blade-type rotor. Rotor speed and blending temperature were kept at 50 rpm and 100 °C respectively and reaction time was 15 min. Before blending, the starch was dried in an oven at 105 °C for 24 h. The mass ratios of starch to PCL were set at 10/90, 20/80, 30/70, 40/60, and 50/50. After blending, the composites were pressed into 1 mm-thick plate using a hydrolytic press at 140 °C and were put into a dryer for cooling. The cooled plates were then made into standard specimens for further characterization.

2.3. Characterization of blends

2.3.1. NMR/FTIR/DSC analysis

For ^{1}H NMR analysis, the sample was first dissolved in $CDCl_3$ and sealed in an NMR tube (10 mm O.D.). Then, after being degassed, analysis was performed on a Bruker AMX400 ^{1}H NMR spectrometer with conditions of 100 MHz, 30° pulse and 4 s cycle time. Infrared spectra of the thin-film samples were obtained using a BIO-RAD FTS-7PC type FTIR spectrophotometer, and melting temperature (T_m) and fusion heat (δH_f) were determined via a TA instruments 2010 DSC sys-

tem. For the DSC tests, sample weight ranged from 4 to 6 mg, and temperature from −30 to +120 °C, with a heating rate of 10 °C/min.

2.3.2. Composite morphology

After mechanical analysis, plates were treated with hot water at 80 °C for 24 h, then coated with gold, and their morphology observed via a Hitachi Microscopy Model S-1400 scanning electron microscope.

2.3.3. Mechanical property tests

Following the ASTM D638 method, a mechanical tester (Model LLOYD, LR5K type) was used to measure tensile strength and elongation at break. For each sample, a mean value was obtained from five measurements taken at a crosshead speed of 20 mm/min.

2.3.4. Water absorption

Samples for measuring water absorption were in the form of 75×25 mm film strips (150±5 μm thickness) following the ASTM D570-81 method. The samples were dried in a vacuum oven at 50±2 °C for 8 h, cooled in a desiccator and then immediately weighed to the nearest 0.001g (this weight designated as W_c). Thereafter, the conditioned samples were immersed in distilled water, maintained at 25±2 °C, for the 6-week test period. During this period, they were removed from the water at 1-week intervals, gently blotted with tissue paper to remove excess water on the surface, immediately weighed to the nearest 0.001 g (designated as W_w), and returned to the water. Each W_w was an average value obtained from three measurements. The percentage increase of water (in weight) was calculated to the nearest 0.01% as follows:

$$\%W_f = \frac{W_w - W_c}{W_c} \times 100$$

where W_f is the final percentage increase in weight of the tested samples.

2.3.5. Biodegradation studies

Biodegradability of the samples was studied by evaluating weight loss of blends over time in a soil environment. Samples of 30×30×1 mm were weighed and then buried in boxes of alluvial-type soil, obtained in March 2001 from farmland topsoil before planting. The soil was sifted to remove large clumps and plant debris. Procedures used for soil burial were as those described by Chandra and Rustgi [18]. Soil was maintained at approximately 20% moisture in weight and samples were buried at a depth of 15 cm. A control box consisted of only samples and no soil. The buried samples were dug out once a month, washed in distilled water, dried in a vacuum oven at 50±2 °C for 24 h and, before evaluation, equilibrated in a desiccator for at least a day. The samples were then weighed before returning them to the soil.

3. Results and discussion

3.1. Characterization of PCL-g-MAH/starch

The outcome of grafting MAH onto PCL was investigated using FTIR. Fig. 1(A) and (B) shows the FTIR spectra of unmodified PCL and PCL-g-MAH, respectively. The characteristic peaks of PCL [16,19] at 3300–

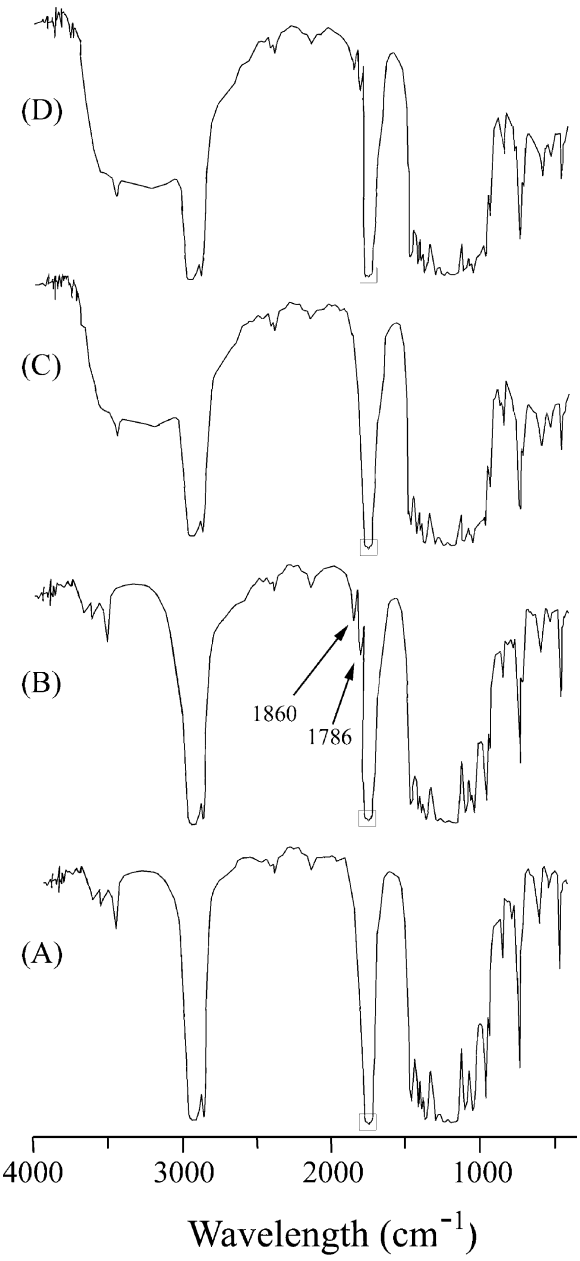

Fig. 1. FTIR spectra of pure PCL and blends. [(A): pure PCL; (B): PCL-g-MAH; (C): PCL/starch (20 wt.%); (D): PCL-g-MAH/starch (20 wt.%).].

3700, 1737, 1725, 850–1480 and 720 cm^{-1} all appeared in both polymers, while extra peaks at 1786 and 1860 cm^{-1} were observed in PCL-g-MAH. Yu et al. [20] indicated that peaks of FTIR spectra at 1781 and 1857 cm^{-1} represent anhydride functional groups of maleic anhydride, as have others [18,21,22]. We were therefore able to confirm that the discernible shoulder in the modified PCL 1786 and 1860 cm^{-1}, based on free acids, demonstrated grafting of MAH onto PCL.

Fig. 2 shows the ^{1}H-NMR spectra of unmodified PCL [Fig. 2(A)] and PCL-g-MAH [Fig. 2(B)]. For unmodified PCL, we found that the hydrogen peaks only appeared at five δ values (1: $\delta = 4.01$ ppm; 2: $\delta = 1.48$ ppm; 3: $\delta = 1.25$ ppm; 4: $\delta = 1.56$ ppm; 5: $\delta = 2.15$ ppm), a similar outcome to other works [23,24]. The spectrum of PCL-g-MAH showed a sixth peak at $\delta = 1.8$–2.0 ppm and a seventh at $\delta = 2.2$–2.4 ppm. These two extra peaks are supposedly due to the grafting of MAH onto the main or branch chain of the PCL skeleton [22,25,26]. In addition, the FTIR spectra of PCL/starch (20 wt.%) and PCL-g-MAH/starch (20 wt.%) [in Fig. 1(C) and (D)] further showed that the peaks at 3200–3700 cm^{-1}, assigned to O–H bond stretching vibration, were much more intense. This is because the –OH group of starch causes/contributes to the bond stretching vibration [14,18]. Further comparison of the spectra of PCL/starch (20 wt.%) and PCL-g-MAH/starch (20 wt.%) showed a unique absorption peak at 1739 cm^{-1} in PCL-g-MAH/starch [shown in Fig. 1(D)], which was assigned to the ester carbonyl stretching vibration in the copolymer. When the FTIR spectra in the range 1700∼1750 cm^{-1} was expanded, the difference between the spectra of PCL/starch and PCL-g-MAH/starch could be more clearly seen. The expanded spectrum for PCL [shown in Fig. 3(A)] shows how the –C=O stretching vibration appeared as a strong broad band at 1725–1736 cm^{-1}. Wang et al. [19] had obtained a similar result. The PCL/starch spectrum [shown in Fig. 3(C)] showed the same broad absorption band, but PCL-g-MAH/starch exhibited a newly formed peak at 1739cm^{-1} [Fig. 3(D)]. Bikiaris et al. [27] studied LDPE/plasticized-starch compatabilized with PE-g-MA copolymers, and also indicated a band at 1735 cm^{-1}. Appearance of this new absorption peak was perhaps due to the formation of an ester carbonyl functional group via reaction between an –OH group of starch and anhydride carbonyl group of PCL-g-MAH when the two polymers were blended.

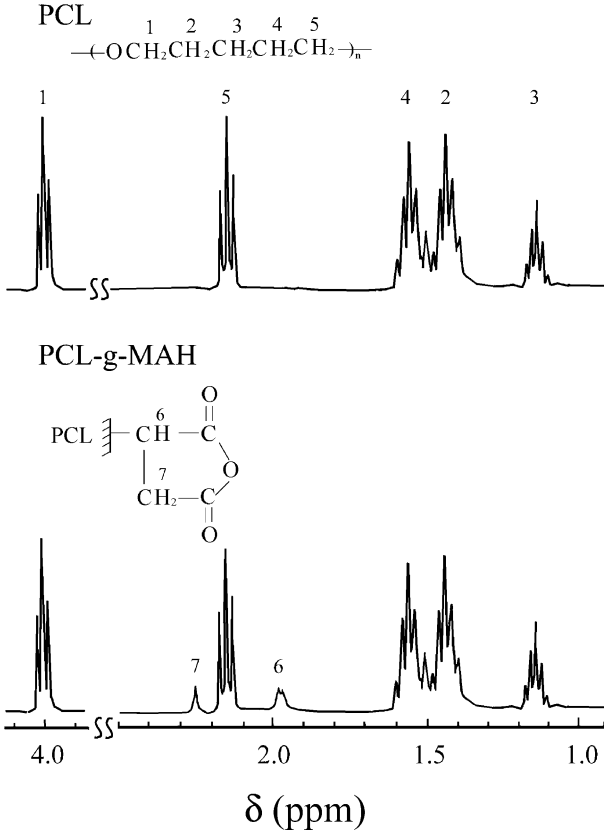

Fig. 2. ^{1}H NMR spectra of unmodified PCL and PCL-g-MAH prepared with 10 wt.% MAH and 0.3 wt.% BPO.

3.2. Torque measurements

The curves of torque vs. mixing time for PCL/starch and PCL-g-MAH/starch blends are presented in Fig. 4. It was observed that the torque value of each blend decreased with increasing starch content and mixing time, and that it approached a stable value when the mixing time was greater than 8 min. We concluded that good mixing had occurred after 15 min. Final torque decreased with increasing starch content because the viscosity of the molten starch was lower than that of molten PCL and molten PCL-g-MAH. Further, the torque response of PCL-g-MAH/starch was significantly lower than that of PCL/starch with the same

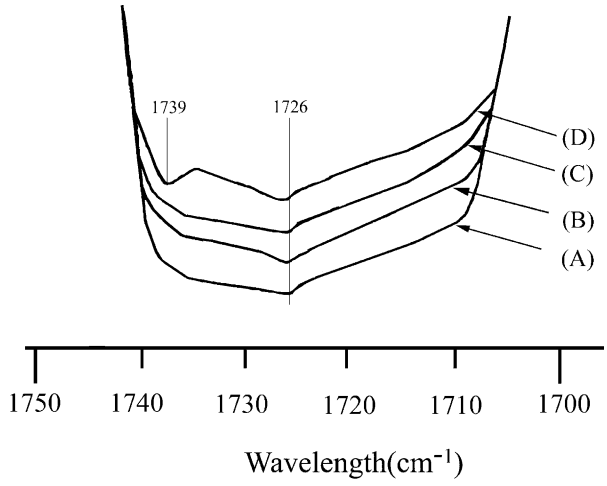

Fig. 3. FTIR spectra in the vicinity of the peaks for C–O and C=O bending deformation for pure PCL and blends with different starch contents. [(A):pure PCL; (B): PCL-g-MAH; (C): PCL/starch (20 wt.%); (D): PCL-g-MAH/starch (20 wt.%).].

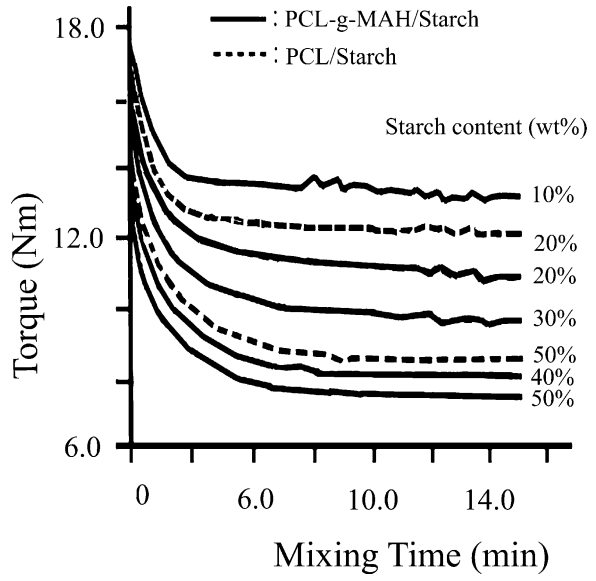

Fig. 4. Torque of PCL/starch and PCL-g-MAH/starch blends at various starch contents.

starch content (20 and 50 wt.%). The improved rheological behavior of PCL-g-MAH/starch was attributed to the conformational change of the starch molecule [28], caused by the previously discussed formation of an ester carbonyl functional group. In the study of Sagar [29], the melt viscosity of esterified starches also decreased with increasing molecular weight of the ester group.

3.3. Differential scanning calorimetry test

Differential scanning calorimetry was used to study the thermal properties of blends. Variations in heat of fusion (δH_f) and melt temperature (T_m) of PCL/starch and PCL-g-MAH/starch were determined from the DSC heating thermograms (not shown here), and the results are presented in Figs. 5 and 6. In Fig. 5, it can be seen that melt temperature decreased with increasing starch content for both PCL/starch and PCL-g-MAH/starch blends, and that the decrease was more noticeable for starch content of up to 20 wt.%. The lower T_m might be caused by starch lowering the melt viscosity of PCL and PCL-g-MAH. The lower melt viscosity of PCL-g-MAH/starch makes this blend easier to process than PCL/starch.

The values of fusion heat (δH_f) of pure PCL and PCL-g-MAH were 72.5 and 52.1 J/g, respectively (Fig. 6). The grafted branches that increased the spacing between the PCL chains and disrupted the regularity of the chain structure [28] might explain the lower fusion heat of PCL-g-MAH. Conversely, as the starch was blended, we found that PCL-g-MAH/starch gave higher ΔH_f values than PCL/starch, with an increment of about 4–10 J/g, a function of the ester carbonyl functional group of PCL-g-MAH. However, it was clear that the ΔH_f value, which indicates percentage crystallinity of blends, of both PCL/starch and PCL-g-MAH/starch decreased as the content of starch was increased. These phenomena were similar to the results of Aburto et al. [28], who studied the properties of octanoated starch and its blends with polyethylene. Marked decrease in crystallinity of PCL/starch blends was probably caused by the increased difficulty in arranging the polymer chain as the starch prohibited the movements of the polymer segments and by the steric effect caused by the hydrophilic character of starch, leading to poor adhesion with the hydrophobic PCL [28,30].

3.4. Composite morphology

To further understand changes in mechanical properties of the composites, the morphology of the polymer was investigated via SEM. In the PCL/starch composites, the matrix is PCL and the dispersed phase is starch. Table 1 tabulates the starch phase size (the average pore diameter) of PCL/starch and PCL-g-

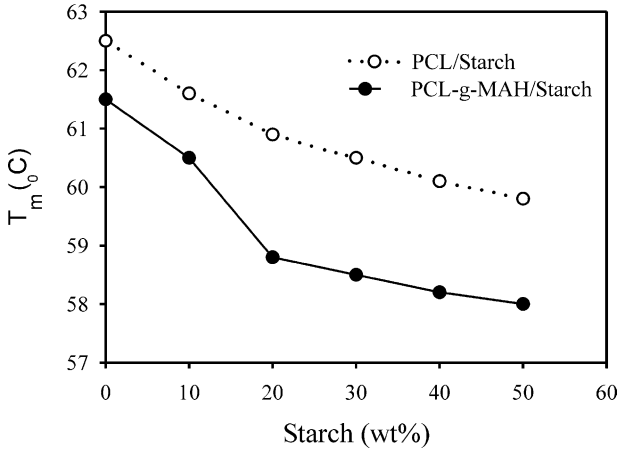

Fig. 5. Melt temperature vs. starch content for PCL/starch and PCL-g-MAH/starch blends.

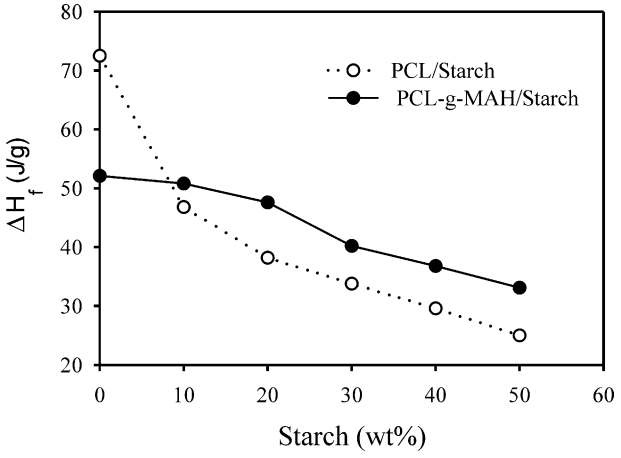

Fig. 6. Fusion heat vs. starch content for PCL/starch and PCL-g-MAH/starch blends.

Table 1
The starch phase size of PCL-g-MAH/starch and PCL/starch blends at different starch contents

Starch (wt.%)	Phase size (μm)	
	PCL/starch	PCL-g-MAH/starch
10	6.5	1.5
20	12.0	2.1
30	15.5	3.3
40	18.0	3.8
50	21.0	4.1

MAH/starch composites. There was fine dispersion and homogeneity of starch in the PCL/starch matrix at starch loading <10 wt.%. For PCL/starch composites, it was found that as starch content increased, the size of the starch phase increased. The large starch phase size, especially that formed in the composite containing 50 wt.% starch, suggests that the adhesion between starch and PCL is very poor and that the two polymers are strongly incompatible [14].

When PCL-g-MAH was added, the size of the starch phase was much decreased compared with the ungrafted equivalent (Table 1). The results in Table 1 show that there was fine dispersion and homogeneity of starch in the PCL matrix for all PCL-g-MAH/starch composites, as the phase size was never greater than 4.1 μm, and was detectable only at higher magnification. This better dispersion arose from the formation of branched and crosslinked macromolecules, since the PCL-g-MAH copolymer has anhydride groups that react with the hydroxyl groups of starch. Because the different parts of the branched and crosslinked macromolecules were all compatible with the polymer phases, this gave them the ability to place themselves in the interface between PCL and starch during melt blending. The result was a reduction in the interfacial tension between the two polymers and a finer distribution of starch in all the grafted composites. Such a scenario was also proposed by Bikiaris [14], who found that a LDPE (LDPE-g-MAH)/starch composite produced smaller pore sizes under tensile disruption.

3.5. Mechanical properties

Fig. 7 shows the effect of starch content on tensile strength and elongation at break for PCL/starch and PCL-g-MAH/starch composites. For PCL/starch composites, tensile strength decreased continuously as starch content increased. It was thus clear that mechanical incompatibility of the two phases was great and would increase with the starch content. Though lower tensile strength at break was observed for PCL-g-MAH composites compared with pure PCL, this decrease was smaller than that of the equivalent uncompatibilized

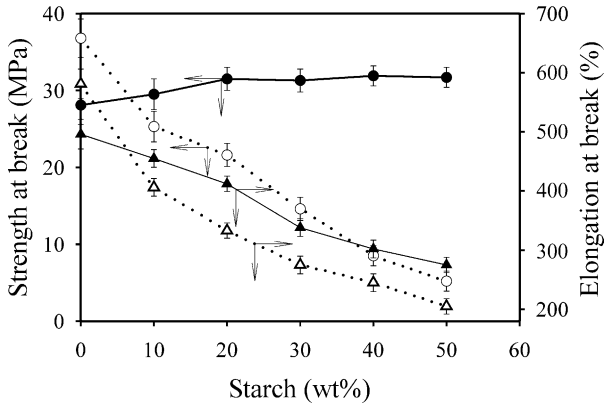

Fig. 7. Tensile strength and elongation at break vs. starch content for PCL-g-MAH and PCL blends. [The solid and dotted lines indicated thePCL-g-MAH and PCL ones, respectively.]

composites. The absolute value of tensile strength at break for all compatibilized composites was noticeably higher than that of their uncompatibilized counterparts. It was also found that the PCL-g-MAH composites provided more stable values of tensile strength when the starch content was <10 wt.%.

Fig. 7 also shows that the PCL-g-MAH composite exhibits a higher elongation at break compared with the uncompatibilized composites, and that the difference increases with increasing starch content. However, compared with the equivalent pure PCL, elongation at break of both composites decreased with increasing starch content. The findings of Bikiaris et al. [13] regarding mechanical properties of LDPE/plasticized-starch containing PE-g-MA compatibilizer were similar to those discussed here. It is evident that the mechanical properties strongly depend on the dispersion and phase size of starch in the PCL matrix. With a smaller dispersed phase, an improvement in mechanical properties, especially in tensile strength, is observed.

3.6. Water absorption

PCL-g-MAH/starch blends exhibited moderately good water resistance and resistance was higher than that of PCL/starch blends at the same starch content (Fig. 8). The increment of water absorption for PCL/starch, compared with the value of PCL-g-MAH/starch, was about 0.9–2%. For both types of blend, the percentage water gain increased with starch content, and it increased slowly over the 6-week test period. These phenomena were similar to the results of Bikiaris and Panayiotou [14]. By studying blends of starch and polyethylene, they deduced that the marked increase in water absorption was probably caused by the increased difficulty in forming polymer chain arrangements as the starch prohibited the movements of the polymer segments, and also that the hydrophilic character of starch led to poor adhesion with the hydrophobic polyethylene

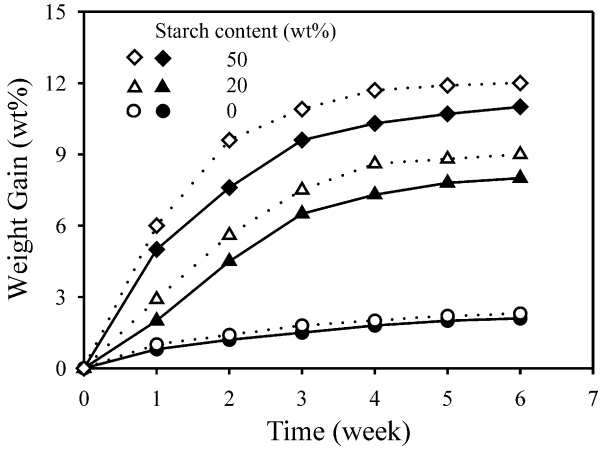

Fig. 8. Percentage weight gain of PCL/starch and PCL-g-MAH/starch blends during water absorption. [The solid and dotted lines indicated the PCL-g-MAH and PCL ones, respectively.].

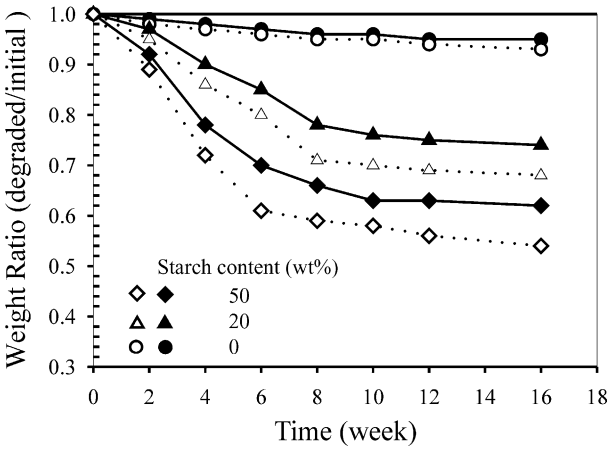

Fig. 9. Weight ratio of PCL/starch and PCL-g-MAH/starch blends exposed to soil environment. [The solid and dotted lines indicated the PCL-g-MAH and PCL ones, respectively.].

(a steric effect). In this study, the comparatively lower water absorption of PCL-g-MAH was caused by the ester carbonyl functional group on that blend.

3.7. Biodegradation under soil environment

Fig. 9 shows changes in weight ratio (degraded sample/initial sample) with time for the PCL/starch and PCL-g-MAH/starch buried in soil. In the soil, water diffused into the polymer sample, causing swelling and enhancing biodegradation. The blends containing a higher percentage of starch (50% starch content) degraded rapidly in the initial 8 weeks, equivalent to the approximate starch content of the blends, and a gradual decrease of weight occurred during the next 8 weeks. The weight loss of PCL/starch and PCL-g-MAH/starch, which indicated the extent of biodegradation of the blends, both increased as the content of starch increased. Further comparison of the two copolymers revealed that PCL-g-MAH/starch had a higher weight ratio, with an increment of about 0.03–0.10. The greater biodegradation of PCL/starch may be caused by the same factors leading to its higher absorption of water. Under the soil environment, the mechanical properties of blends, such as tensile strength and elongation at break, also deteriorated.

4. Conclusions

Compatibility and mechanical properties of a PCL/starch composite were improved by using PCL-g-MAH in place of PCL. The blending of PCL-g-MAH with starch leads to the formation of an ester carbonyl group not present in PCL/starch. This group is responsible for many of the differences in mechanical properties between the two copolymers. While the melt temperature (T_m) of both copolymers decreases with increasing starch content, PCL-g-MAH/starch is more easily processed due to its lower melt temperature and torque requirement. The fusion heat (ΔH_f) of PCL/starch decreased with increasing starch content while that of PCL-g-MAH/starch increased. Increases in starch phase size with increasing starch content demonstrate the poor compatibility between PCL and starch. The improved compatibility between the constituents of PCL-g-MAH/starch is therefore illustrated by the noticeable reduction in starch phase size (being always less than 4.1 μm). Compared with PCL/starch, tensile strength of PCL-g-MAH/starch was enhanced, and elongation at break improved, although these properties worsened in both composites as starch content increased. Although water resistance of PCL-g-MAH/starch was higher than that of PCL/starch, in a soil environment the compatibilized blend showed only a slightly lower biodegradation rate than the uncompatibilized one.

References

[1] Degli-Innocenti F, Bellia G, Tosin M, Kapanen A, Itavaara M. Polym Degrad Stab 2001;73:101.
[2] Ahamed NT, Singhal RS, Kulkarni PR, Kale DD, Pal M. Carbohydr Polym 1996;31:157.
[3] Koenig MF, Huang SJ. Polymer 1995;36:1877.
[4] Ishiaku US, Pang KW, Lee WS, Ishak ZAM. Eur Polym J 2002; 38:393.
[5] Psomiadou E, Arvanitoyannis I, Biliaderis CG, Ogawa H, Kawasak N. Carbohydr Polym 1997;33:227.
[6] Bikiaris D, Pavlidou E, Prinos J, Alric I, Borredon E, Panayiotou C. Polym Degrad Stab 1998;60:437.
[7] Darwis D, Mitomo H, Yoshil F. Polym Degrad Stab 1999; 65:279.
[8] Wang L, Ma W, Gross RA, McCarthy SP. Polym Degrad Stab 1998;59:161.
[9] Oda Y, Asar H, Urakami T, Tonomura K. J Fermentation Bioeng 1995;80:265.
[10] Abou-Zeid DM, Muller RJ, Deckwer WDL. J Biotechnol 2001; 86:113.

[11] Cao A, Okamura T, Ishiguro C, Nakayama K, Inoue Y, Masuda T. Polymer 2002;43:671.
[12] Orhan Y, Buyukgungor H. Int Biodeterioration Biodegrad 2000; 45:49.
[13] Bikiaris D, Prinos J, Koutsopoulos K, Vouroutzis N, Pavlidou E, Frangis N, Panayiotou C. Polym Degrad Stab 1998;59:287.
[14] Bikiaris D, Panayiotou C. J Appl Polym Sci 1998;70:1503.
[15] Dubois P, Krishnan M, Narayan R. Polymer 1999;40:3091.
[16] Avella M, Errico ME, Laurienzo P, Martuscelli E, Raimo M, Rimedio R. Polymer 2000;41:3875.
[17] Gaylord NG, Mehta R, Kumar V, Tazi M. J Appl Polym Sci 1989;38:359.
[18] Chandra R, Rustgi R. Polym Degrad Stab 1997;56:185.
[19] Wang J, Cheung MK, Mi Y. Polymer 2002;43:1357.
[20] Yu ZZ, Ou YC, Qi ZN, Hu GH. J Polym Sci: Part B: Polym Phys 1998;36:1987.
[21] Wang Y, Ji D, Yang C, Zhang H, Qin C, Huang B. J Appl Polym Sci 1994;52:1411.
[22] Wu CS, Liao HT, Lai SM. Polym-Plast Technol Eng 2002; 41:645.
[23] Kim C-H, Cho KY, Park J-K. Polymer 2001;42:5135.
[24] Rutot D, Duquesne E, Ydens I, Degee P, Dubois P. Polym Degrad Stab 2001;73:561.
[25] Russell KE, Kelusky EC, Kingston. J Polym Sci Polym Chem Ed 1988;26:2273.
[26] Shatter TD, Canich JAM, Squire KR. Macromolecules 1998;31:5145.
[27] Bikiaris D, Prinos J, Panayiotou C. Polym Degrad Stab 1997;58:215.
[28] Aburto J, Thiebaud S, Alric I, Bikiaris D, Prinos J, Panayiotou C. Carbohydr Polym 1997;34:101.
[29] Sagar AD, Merril EW. J Appl Polym Sci 1995;58:1647.
[30] Prinos J, Bikiaris D, Theologidis S, Panayiotou C. Polym Eng Sci 1998;38:954.